



# Population Pharmacokinetics and Pharmacodynamics of Fepixnebart (LY3016859) and Epiregulin in Patients with Chronic Pain

Douglas E. James<sup>1</sup> · Jason Bailey<sup>2</sup> · Jan-Stefan van der Walt<sup>3,4</sup> · Julia Winkler<sup>4</sup> · Rik Schoemaker<sup>4</sup>

Accepted: 30 March 2025 / Published online: 23 April 2025  
© The Author(s) 2025

## Abstract

**Background and Objective** Fepixnebart (LY3016859), a humanized immunoglobulin G4 monoclonal antibody with high binding affinity to epiregulin and tumor growth factor- $\alpha$ , is being developed as a novel analgesic to treat broad-spectrum chronic pain. Early phase clinical studies demonstrated fepixnebart has nonlinear pharmacokinetics in healthy subjects and patients with diabetic nephropathy. This population pharmacokinetic analysis used data from three 26-week, phase 2, proof-of-concept studies in osteoarthritis, diabetic peripheral neuropathic pain (DPNP), and chronic low back pain (CLBP) to characterize the pharmacokinetics of fepixnebart and predict its target engagement by epiregulin. Covariate relationships were also assessed.

**Methods** Population analysis was performed using nonlinear mixed-effects modeling software. Covariate relationships were explored graphically by plotting potential covariates versus parameters of interest. Simulated target engagement was predicted using the phase 2 dose regimen for fepixnebart (750 mg intravenous starting dose, followed by 500 mg every 2 weeks).

**Results** The median simulated target engagement at 2 weeks after the last dose of fepixnebart was predicted to be 92.0%, with 90% of predictions between 86.0 and 96.2% and 68.5% of subjects predicted to exhibit target engagement exceeding 90%.

**Conclusions** The phase 2 dose regimen is adequate to test the analgesic effect of fepixnebart in patients with osteoarthritis, DPNP, and CLBP. In the final model, female sex and higher glomerular filtration rate were associated with higher clearance, female sex was associated with larger volume of distribution of the central compartment ( $V_c$ ) than male sex, and DPNP was associated with lower  $V_c$  than CLBP. There were no significant effects on the concentration of fepixnebart at which its effect on epiregulin is half-maximal ( $EC_{50}$ ).

**Trail Registry** ClinicalTrials.gov: NCT04529096, NCT04476108, and NCT04456686.

## 1 Introduction

Chronic pain is a highly prevalent condition with a huge societal impact. In 2016, an estimated 20.4% of the adult population in the USA experienced chronic pain, defined as pain on most days, or every day in the past 6 months, on the basis of data from the National Health Interview Survey [1].

For several years, clinicians have published case reports or case series on the analgesic benefit of epidermal growth factor receptor (EGFR) antibody antagonists or EGFR

### Key Points

Phase 2 studies showed that the dosing regimen for fepixnebart (LY3016859), a new drug being developed to treat various types of chronic pain, was effective in engaging its target, with a high percentage of subjects showing strong engagement.

Epiregulin, a ligand for EGFR, is a promising target for treating chronic pain due to its role in persistent EGFR pathway activation.

✉ Douglas E. James  
james\_douglas\_e@lilly.com

<sup>1</sup> Global PK/PD and Pharmacometrics, Eli Lilly and Company Corporate Center, Indianapolis, IN 46285, USA

<sup>2</sup> LEM CAG, Eli Lilly and Company, Indianapolis, IN, USA

<sup>3</sup> Former Employee of Global PK/PD and Pharmacometrics, Eli Lilly and Company, Indianapolis, IN, USA

<sup>4</sup> Occams Coöperatie UA, Amstelveen, The Netherlands

tyrosine kinase inhibitors in oncology patients that were independent of the oncolytic efficacy of these agents [2, 3]. These data suggest the EGFR pathway is involved in the pathogenesis of neuropathic pain. However, targeting the receptor with an anti-EGFR antibody or EGFR tyrosine kinase inhibitors is associated with a high incidence of

gastrointestinal and dermatological adverse reactions, limiting their potential use in the non-oncological population with chronic pain.

Ligands that bind and activate EGFR include epiregulin, transforming growth factor- $\alpha$  (TGF $\alpha$ ), epidermal growth factor, heparin-binding epidermal-like growth factor, betacellulin, amphiregulin, and epigen [4]. Two of the EGFR ligands, TGF $\alpha$  and epiregulin, are unique in that they fail to induce receptor degradation and thus promote receptor recycling and persistent EGFR pathway activation [5]. Epiregulin exists in a soluble form in the blood in addition to membrane-bound in the tissues. Fepixnebart (LY3016859)-bound epiregulin was used as the target engagement biomarker.

Fepixnebart is a humanized immunoglobulin G4 monoclonal antibody (Mab) with high binding affinity to epiregulin and TGF $\alpha$ . It is being developed as a novel analgesic for the treatment of broad-spectrum chronic pain, including diabetic peripheral neuropathic pain (DPNP), signs and symptoms of osteoarthritis (OA), and chronic low back pain (CLBP). In early phase clinical studies, fepixnebart was shown to have nonlinear pharmacokinetics (PK), likely due to target-mediated drug disposition, in healthy subjects and in patients with diabetic nephropathy, as well as a high frequency of antidrug antibodies (ADAs) that was not found to impact PK [6].

The objective of this population pharmacokinetic/pharmacodynamic (PKPD) analysis was to characterize the PK and exposure–response relationship in participants with chronic pain. We also sought to determine whether the phase 2 dose regimen (750 mg intravenous [IV] starting dose, followed by 500 mg every 2 weeks [Q2W]) would achieve the required level of target engagement in patients (90% at trough).

## 2 Methods

### 2.1 Dosing

Fepixnebart concentrations (PK) and fepixnebart-bound epiregulin (pharmacodynamic [PD]) data were available from three phase 2, proof-of-concept, randomized, double-blind, placebo-controlled studies in OA (NCT04456686), DPNP (NCT04476108), and CLBP (NCT04529096) that lasted for 26 weeks and included an 8-week double-blinded treatment period and an 18-week follow-up period. Participants were randomly assigned to fepixnebart or placebo in a 2:1 ratio. Participants received an IV infusion Q2W for a total of 4 infusions; the starting dose for LY-treated participants was 750 mg and subsequent doses were 500 mg. The dose level and duration were selected

on the basis of available toxicology, safety, PK, and PD. The dose regimen is expected to achieve an exposure such as the 750 mg every 3 weeks dosing regimen tested in a previous clinical study. While the degree of target engagement required for analgesic efficacy had not been established in the clinic, the dosing regimen was expected to reach steady state within a month and achieve > 90% engagement of soluble target in more than 50% of patients by week 4 and to maintain adequate therapeutic concentrations on the basis of PK/PD analyses. Because these were the first proof-of-concept studies in chronic pain, the strategy was to take the highest dose that demonstrated appropriate target engagement, safety, and tolerability from the phase 1 studies.

### 2.2 PKPD Measurements

Samples were collected for PK prior to dosing and within 15 min post-infusion at study weeks 0, 2, 4, and 6, as well as at weeks 8, 12, 16, and 26. Epiregulin samples were collected prior to dosing at weeks 0, 2, and 4, as well as at weeks 8, 12, 16, and 26.

Samples for fepixnebart were analyzed using an enzyme-linked immunosorbent assay with an anti-idiotypic antibody binding the variable region of fepixnebart, thus the assay measured free fepixnebart capable of binding the target. The lower limit of quantification was 5 ng/mL and the upper limit of quantification was 120 ng/mL; samples with higher concentrations were diluted to accommodate the assay range. The fepixnebart ADA assay was a Meso-Scale Discovery-based affinity capture elution bridging assay. The epiregulin biomarker assay is an electrochemiluminescence immunoassay performed on the Meso-Scale Discovery platform. Fepixnebart-bound epiregulin in patient serum was captured on an anti-epiregulin-coated plate and detected using a ruthenium-labeled anti-idiotypic antibody that binds fepixnebart. The lower limit of quantification was 78 pg/mL and the upper limit of quantification was 80,000 pg/mL.

### 2.3 Population PK and PD Models

The population analysis was performed using the nonlinear mixed-effects modeling software NONMEM Version 7.5.0 [7] supplemented with Perl-speaks-NONMEM (PsN; version 4.6.0 [8]). R software Version 4.0.5 was used for data management, simulation using the RxODE package [9], evaluation of goodness-of-fit, and model evaluation. Parameter estimation was performed in NONMEM using first order conditional estimation with the INTERACTION option.

A simultaneous modeling approach was used to develop the PKPD model, where both PK and PD parameters were estimated together. The population PKPD modeling process is detailed below.

## 2.4 PK and PD Modeling

Analysis of the pooled PK and PD data available from the phase 2 studies indicated that fepixnebart profiles could be described with a parallel linear/Michaelis–Menten elimination model:

$$\frac{dLY_C}{dt} = K_{21} \cdot LY_P - K_{12} \cdot LY_C - \frac{V_{max} \cdot LY_C/V_c}{K_m + LY_C/V_c} - CL \cdot LY_C/V_c$$

$$\frac{dLY_P}{dt} = -K_{21} \cdot LY_P + K_{12} \cdot LY_C$$

where  $LY_C$  and  $LY_P$  are fepixnebart amounts in the central and peripheral compartments, respectively,  $CL$  is the linear clearance of fepixnebart (reflective of normal immunoglobulin  $G$  catabolism as well as elimination related to binding to soluble epiregulin),  $V_{max}$  and  $K_m$  are Michaelis–Menten clearance parameters describing the target-mediated drug disposition related to rapid tissue binding to pro-epiregulin,  $V_c$  is the volume of the central compartment, and  $K_{12}$  and  $K_{21}$  are rate constants driving exchange between the central and peripheral compartments.

The influence of fepixnebart on epiregulin was described with an indirect response model including a sigmoid- $E_{max}$  relationship between fepixnebart concentration and reduction of epiregulin elimination:

$$\frac{d\text{Epiregulin}}{dt} = K_{syn} - \text{Epiregulin} \cdot K_{deg} \cdot \left( 1 - \frac{E_{max} \cdot LY_C/V_c^{Hill}}{EC_{50}^{Hill} + LY_C/V_c^{Hill}} \right)$$

where  $K_{syn}$  describes the endogenous rate of epiregulin synthesis and  $K_{deg}$  quantifies the rate of epiregulin degradation, modified in the presence of fepixnebart. A schematic representation of the PK-PD model structure is provided in Fig. 1.

Preliminary assessment suggested that suppression was very pronounced, and the maximal effect of fepixnebart on epiregulin ( $E_{max}$ ) could therefore be fixed to one.

The Hill equation component describes the fepixnebart-inhibited elimination of epiregulin. If the fepixnebart-induced elimination of epiregulin is assumed to be the same as the target engagement process, then the Hill equation describes the fepixnebart target engagement:

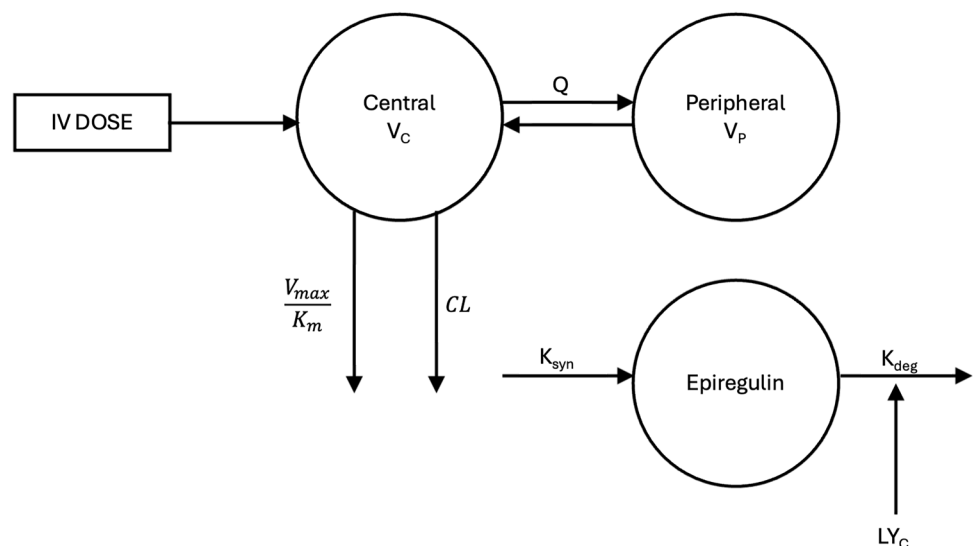
$$\text{Target engagement} = \frac{E_{max} \cdot LY_C/V_c^{Hill}}{EC_{50}^{Hill} + LY_C/V_c^{Hill}}$$

The influence of body size on the PK of fepixnebart was incorporated by implementing allometric scaling of the linear PK parameters on body weight a priori using the following equation:

$$PAR_i = \theta_1 \cdot \left( \frac{\text{Body weight}_i}{70} \right)^{\theta_2} \cdot e^{\eta_i}$$

where  $\theta_1$  is the population value of the estimated PK parameter,  $PAR_i$  the individual-specific realization for the  $i$ th subject with the value of body weight scaled to 70 kg. The parameter  $\theta_2$  is the scaling parameter for the body weight range, which can be either fixed to allometric values or freely estimated. If allometric scaling

**Fig. 1** Model schematic for the final PK and PK-PD model



principles are applied,  $\theta_2$  takes on specific (fixed) values for the influence of body size; these values are 0.75 for CL and inter-compartmental clearance ( $Q$ ), and 1 for  $V_c$  and the volume of the peripheral compartment ( $V_p$ ) [10]. A model with all four exponents estimated freely (on CL,  $Q$ ,  $V_c$ , and  $V_p$ ) was compared with a model with all four exponents fixed to their theoretical values. On the basis of the outcome, and only if associated with a large drop in objective function value (OFV), it was decided to estimate one or more of the coefficients freely.

## 2.5 Covariates

Covariates for PK were investigated for their effect on the CL and  $V_c$  of fepixnebart, and covariates for the PKPD relationship were investigated for their effect on the concentration of fepixnebart at which its effect on epiregulin is half-maximal ( $EC_{50}$ ).

Potential covariate relationships were explored graphically by plotting potential covariates versus parameters of interest. Graphical exploration procedures were only relied upon if the degree of  $\eta$ -shrinkage in the parameters was reasonably low (less than 30%) [11]. The degree of shrinkage in model parameters is presented in this manuscript.

The following demographic covariates were considered in the analysis for their effects on fepixnebart PK and PKPD:

- body weight at baseline
- sex
- age at baseline
- renal function estimated by the six-variable Modification of Diet in Renal Disease Study equation (MDRD-6) [12]
- time-varying occurrence of the presence of ADAs (PK only), and
- disease population (OA, CLBP, and DPNP).

The following procedure was used to assess covariates, but deviation from this procedure was allowed when dictated by the data. Effects of single covariates on CL,  $V_c$ , and  $EC_{50}$  were implemented in separate models and the resulting estimates were presented in a forest plot [13]. On the basis of the results, a subset of covariates demonstrating a statistically significant effect was used to create a full covariate model with only the selected covariates included. The full covariate model was then subjected to an automated stepwise covariate modeling procedure using backward deletion only, as implemented in PsN [8]. Backward deletion was performed using a  $p$ -value of  $< 0.001$  as the selection criterion.

## 2.6 Model Evaluation

Standard continuous-data goodness-of-fit plots were used to assess the adequacy of PK models. Simulation-type diagnostics such as visual predictive checks (VPCs) [14] were additionally used in model assessment, and to determine whether the observed population profiles could be simulated using the models. To perform VPCs, 1000 studies were simulated with a structure identical to the study analyzed; population parameters for each simulated study were sampled from a multivariate normal distribution using the estimated population theta estimates and their estimated interindividual variability (IIV). Individual profiles were then simulated using the sampled individual parameters and the analysis model.

To assess parameter precision and derive confidence intervals, the sampling importance resampling procedure was applied to the final PK model as implemented in PsN. Use of the sampling importance resampling procedure provides an estimate of parameter precision that is reportedly superior to traditional bootstrap approaches [15].

## 2.7 Model Application (Simulation)

The main deliverable from the PKPD model was the predicted soluble target engagement for epiregulin. Individual profiles were simulated for the LY3016859 concentrations, epiregulin concentrations, and predicted percentage target engagement, using individual empirical Bayes estimates of the PK and PKPD parameters, and using a standard dosing schedule (first dose of 750 mg, followed by three 500 mg doses, each 2 weeks apart, infused over 1 h), and these profiles were summarized using median, 5th and 95th percentiles to document the range of predicted outcomes over time. Additionally, the predicted percentage target engagement at week 8 (2 weeks after the final dose) was summarized.

## 2.8 Immunogenicity

Samples were tested at Nexelis (Seattle, WA) for anti-LY3016859 using an established electrochemiluminescence immunoassay method [16].

## 3 Results

### 3.1 Patient Characteristics

The population PK and PD dataset included data from 386 participants whose ages ranged from 20 to 84 years at study

entry and who weighed between 47 and 148 kg. The range and mean values of age, weight, and glomerular filtration rate (GFR) by pain indication are provided in Table 1.

### 3.2 Immunogenicity

In the fepixnebart groups, a total of 70 participants (27 [27.8%] in CLBP, 28 [34.1%] in DPNP, and 15 [19.7%] in OA) developed treatment-emergent ADAs during the studies. With the exception of one participant in study NP, nearly all ADAs observed were neutralizing (69/70 [98.6%]). The majority of ADA titers were low, with the highest reported titer being 1:2560.

### 3.3 PK and PD Results

The combined PKPD dataset contains 2444 fepixnebart concentrations and 2436 fepixnebart-bound epiregulin concentrations. The PK time course data were well described by a two-compartment model with a parallel linear/Michaelis–Menten elimination. Allometric scaling was applied to the clearance (CL and  $Q$ ) and volume ( $V_c$  and  $V_p$ ) parameters, where both fixed and estimated exponents were evaluated. IIV was estimated on all parameters except for  $Q$ .

The effects on exposure were quantified as fold-change on average concentration by using the inverse of CL, on the assumption that linear clearance is primarily responsible for average steady state concentration. The estimates of single covariate effects on CL with 95% confidence intervals are shown using forest plots in Fig. 2. Results of single covariate runs are presented in Table 2.

Single covariate effects were similarly assessed on  $V_c$  and  $EC_{50}$ . Significant single covariate effects of sex and GFR were found on CL, significant single covariate effects of sex and DPNP were found on  $V_c$ , and a significant single covariate effect of sex was found on  $EC_{50}$ . These covariates

were all included in a full starting model and subjected to a backward stepwise covariate modeling procedure (with a critical value of  $p < 0.001$ ) to detect which covariates in a joint covariate model would remain.

After the final covariate model was obtained, the model was refined. In the first step, allometric exponents of  $V_c$  and  $V_p$  were estimated, and resulted in a drop in OFV ( $\Delta$ OFV) of 31.18. In the subsequent model, the Hill factor was also estimated. This resulted in a highly significant  $\Delta$ OFV of 296.95 points compared with the previous model. Estimation of IIV on the Hill factor led to another drop in OFV of 54.

In the final model, incorporating the effect of body weight on CL,  $Q$ ,  $V_c$ , and  $V_p$  with estimated allometric exponents, female sex, and higher GFR were associated with higher CL (resulting in lower exposure), female sex was associated with a larger  $V_c$  than male sex, and DPNP was associated with a lower  $V_c$  than CLBP. There were no significant effects on  $EC_{50}$ . The NONMEM estimates for the final population PKPD model are provided in Table 3.

Visual predictive checks (using the automatic binning algorithm K-means clustering in PsN) were performed for the final population PKPD model to investigate whether model simulations correspond to observed medians and ranges for the entire population, stratified by fepixnebart concentrations or epiregulin concentrations. Figures 3 and 4 demonstrate that there was adequate correspondence between 5th, 25th, 50th (median), 75th, and 95th percentiles of the observed data and corresponding simulated quantiles for both fepixnebart and epiregulin, respectively.

### 3.4 Model Application

Simulated individual profiles for PKPD and target engagement were summarized using the median and 5th and 95th percentiles to document the range of predicted outcomes over time in Fig. 5. Additionally, predicted median target engagement at week 8 (2 weeks after the

**Table 1** Demographic characteristics

Characteristic	CLBP ( $N = 149$ )	DPNP ( $N = 124$ )	OA ( $N = 113$ )	Overall ( $N = 386$ )
Sex, $n$ (%)				
Female	83 (55.7)	49 (39.5)	73 (64.6)	205 (53.1)
Male	66 (44.3)	75 (60.5)	40 (35.4)	181 (46.9)
Age, years	54.5 (20–80)	62.1 (34–84)	62.9 (43–82)	59.4 (20–84)
Weight, kg	88.1 (47–127)	94.2 (51.2–148)	89.4 (57.2–135)	90.4 (47–148)
GFR at baseline, mL/min/1.73 m <sup>2</sup>	91.8 (63.0–138)	88.1 (52.0–126)	84.8 (55.0–118)	88.6 (52.0–138)

Demographic characteristics are presented as mean (range) unless otherwise indicated

CLBP chronic lower back pain, DPNP diabetic peripheral neuropathic pain, GFR body surface area adjusted glomerular filtration rate calculated using the six-variable Modification of Diet in Renal Disease Study equation, OA osteoarthritis



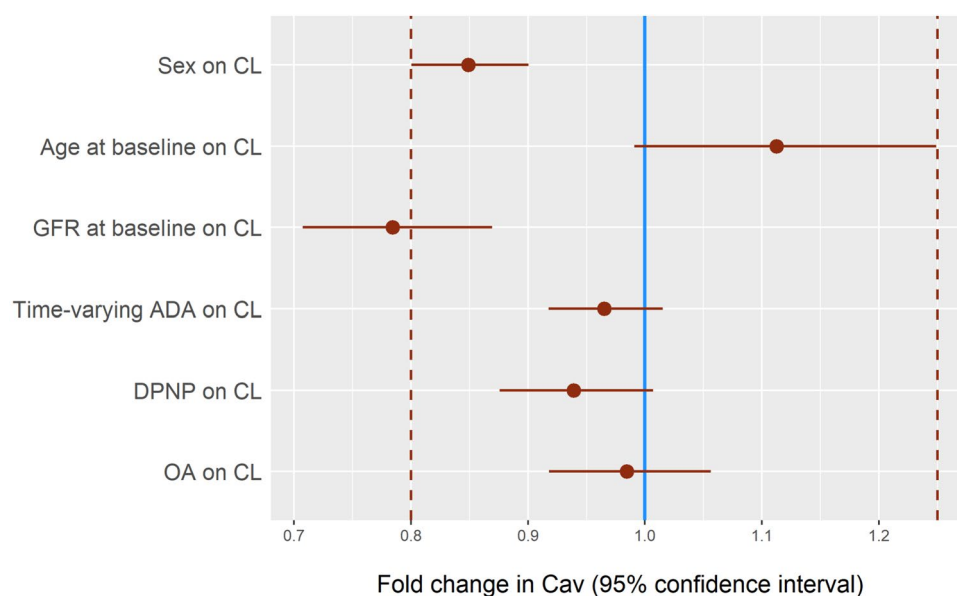


**Fig. 2** Forest plot for single covariate effects on fold change in fepixnebart Cav with 95% confidence intervals. *ADA* occurrence of antidrug antibodies during treatment, *Cav* average concentration over 24 h, *DPNP* diabetic peripheral neuropathic pain relative to chronic low back pain, *GFR* body surface area adjusted glomerular filtration rate using the six-variable Modification of Diet in Renal Disease

Study equation, *OA* osteoarthritis knee pain relative to chronic low back pain, *SEX* females relative to males. Red lines indicate the limits associated with 0.8- to 1.25-fold change in Cav. Continuous covariates (age, GFR) are scaled to estimate the fractional change across 95% of the covariate range

**Table 2** NONMEM objective function values (OFV) for the single covariate runs

Run	Model	OFV	Delta
run100	Base model	43614.53	
run300	Covariate sex on CL	43585.94	– 28.59 versus run100 ( $p < 0.0001$ )
run301	Covariate age on CL	43611.20	– 3.33 versus run100 ( $p = 0.0680$ )
run302	Covariate GFR at baseline on CL	43596.26	– 18.27 versus run100 ( $p < 0.0001$ )
run304	Covariate time-varying ADAs on CL	43611.80	– 2.73 versus run100 ( $p = 0.0983$ )
run305	Covariate disease on CL	43611.19	– 3.34 versus run100 ( $p = 0.1881$ )
run306	Covariate sex on $EC_{50}$	43606.92	– 7.61 versus run100 ( $p = 0.0058$ )
run307	Covariate age on $EC_{50}$	43614.05	– 0.48 versus run100 ( $p = 0.4888$ )
run308	Covariate GFR at baseline on $EC_{50}$	43612.58	– 1.95 versus run100 ( $p = 0.1627$ )
run310	Covariate disease on $EC_{50}$	43607.72	– 6.81 versus run100 ( $p = 0.0332$ )
run311	Covariate sex on $V_c$	43602.98	– 11.55 versus run100 ( $p = 0.0007$ )
run312	Covariate age on $V_c$	43611.99	– 2.54 versus run100 ( $p = 0.1108$ )
run313	Covariate GFR at baseline on $V_c$	43612.96	– 1.57 versus run100 ( $p = 0.2105$ )
run315	Covariate time-varying ADAs on $V_c$	43614.51	– 0.02 versus run100 ( $p = 0.9004$ )
run316	Covariate disease on $V_c$	43603.57	– 10.95 versus run100 ( $p = 0.0042$ )

ADAs antidrug antibodies, CL clearance,  $EC_{50}$  fepixnebart concentration at 50% effect on epiregulin, GFR body surface area adjusted glomerular filtration rate calculated using the six-variable Modification of Diet in Renal Disease Study equation,  $V_c$  central volume of distribution

final dose) for the simulations was 92.0%, with 90% of predictions between 86.0 and 96.2% and with 68.5% of subjects predicted to have a target engagement of over 90%.

## 4 Discussion

A PKPD model for fepixnebart and epiregulin (a ligand that binds and activates EGFR) was developed using data collected in phase 2 studies to assess fepixnebart for the

**Table 3** NONMEM parameter estimates for the final population PKPD model

Parameter	Estimate (95% CI) <sup>a</sup>	RSE	IIV	Shrinkage
CL, mL/h <sup>b,c</sup>	6.72 (6.43, 7.04)	2.9%	21.2%	20.8%
V <sub>c</sub> , L <sup>b,d</sup>	2.42 (2.31, 2.53)	2.4%	17.8%	27.0%
Q, mL/h <sup>b</sup>	12.7 (10.3, 16.6)	20.4%		
V <sub>p</sub> , L <sup>b</sup>	2.06 (1.92, 2.23)	6.4%	16.4%	40.7%
V <sub>max</sub> , µg/h	41.5 (36.2, 47.5)	7.8%	27.0%	53.8%
K <sub>m</sub> , mg/L	0.966 (0.751, 1.19)	13.7%	26.6%	76.4%
EC <sub>50</sub> MAb effect on epiregulin, mg/L	3.42 (3.11, 3.75)	5.9%	19.5%	65.7%
Baseline epiregulin, pg/mL	278 (270, 285)	1.6%	24.9%	6.8%
K <sub>deg</sub> epiregulin, /h	0.0234 (0.0222, 0.0246)	3.1%	26.2%	42.7%
Hill factor effect on epiregulin	0.723 (0.697, 0.748)	2.0%	14.3%	36.1%
Allometric exponent of WT on CL <sup>b</sup>	1.06 (0.926, 1.21)	9.7%		
Allometric exponent of WT on Q <sup>b</sup>	2.81 (2.04, 3.56)	27.7%		
Allometric exponent of WT on V <sub>c</sub> <sup>b</sup>	0.623 (0.510, 0.736)	9.4%		
Allometric exponent of WT on V <sub>p</sub> <sup>b</sup>	1.06 (0.827, 1.28)	22.2%		
GFR on CL <sup>b,c</sup>	1.23 (1.11, 1.36)	25.1%		
Sex on CL <sup>b,c</sup>	1.17 (1.10, 1.23)	19.2%		
Sex on V <sub>c</sub> <sup>b,d</sup>	1.18 (1.13, 1.23)	16.0%		
DPNP on V <sub>c</sub> <sup>b,d</sup>	0.903 (0.857, 0.955)	29.5%		
OA on V <sub>c</sub> <sup>b,d</sup>	1.01 (0.952, 1.07)	408.2%		
RUV LY3016859, %	13.8 (13.3, 14.3)	3.7%		14.3%
RUV Epiregulin, %	18.1 (17.4, 18.8)	3.6%		14.1%

CL clearance, DPNP diabetic peripheral neuropathic pain, EC<sub>50</sub> fepixnebart concentration at 50% effect on epiregulin, GFR body surface area adjusted glomerular filtration rate calculated using the six-variable Modification of Diet in Renal Disease Study equation, IIV interindividual variability, K<sub>deg</sub> epiregulin degradation rate in absence of LY3016859, K<sub>m</sub> fepixnebart concentration at 50% V<sub>max</sub>, OA osteoarthritis, Q inter-compartmental clearance, V<sub>c</sub> central volume of distribution, V<sub>max</sub> maximum Michaelis–Menten elimination rate, V<sub>p</sub> volume of the peripheral compartment, RSE root mean square error, RUV proportional residual unexplained variability (residual error). Shrinkage calculated using the standard deviation.

<sup>a</sup>95% CI from sampling importance resampling (SIR)

<sup>b</sup>Allometric scaling with weight (for a reference individual of 70 kg) was used for the CL, Q, V<sub>c</sub>, and V<sub>p</sub>

<sup>c</sup>CL =  $e^{\log(6.72) + 0.21 \times \frac{\log(\frac{GFR}{88})}{\log(119) - \log(65)} + CLSEX + 1.06 \times \log(\frac{WT}{70})}$ , where WT is body weight and 88 is the median GFR and 65–119 is the 95% percentile range of the GFR data and CLSEX = 0 for male and 0.153 for female patients

<sup>d</sup>V<sub>c</sub> =  $e^{\log(2.42) + VCSEX + VCSTUDY + 0.623 \times \log(\frac{WT}{70})}$ , where WT is the body weight, VCSEX = 0 for male and 0.162 for female patients, and VCSTUDY = 0, −0.102, 0.00735 for patients with CLBP, DPNP, and OA patients, respectively

treatment of broad-spectrum chronic pain in OA, CLBP, and DPNP. The model predicted median target engagement of soluble epiregulin at week 8 (2 weeks after the last dose of fepixnebart) to be 92.0%, with 90% of predictions between 86.0 and 96.2% and 68.5% of subjects predicted to have target engagement > 90%.

The dose regimen for the phase 2 studies consisted of a 750 mg IV starting dose followed by a 500 mg maintenance dose Q2W. This dose regimen was supported by a PKPD model developed using PK and epiregulin data from early phase clinical studies in healthy subjects and in patients with diabetic nephropathy. These studies included a wide dose range: single doses of 0.1, 1, 10, 50, 250, and 750 mg IV,

and multiple doses of 10, 50, 100, 250, and 750 mg IV every 3 weeks. In healthy subjects and in patients with diabetic nephropathy, the PK of fepixnebart was nonlinear, likely due to target-mediated drug disposition which was attributed to the target engagement of membrane-bound epiregulin/TGFα [6]. The dose regimen for the phase 2 studies had to provide sufficient fepixnebart exposure to saturate newly synthesized pro-ligands and avoid target-mediated drug disposition and maximize the drug effect by binding all available soluble epiregulin and prevent activation of EGFR. The level of epiregulin soluble target engagement for analgesic effect in humans is unknown. Soluble target engagement > 90% at 4 and 8 weeks after starting fepixnebart was considered

**Fig. 3** Linear scale (a) and log scale (b) of the VPC for fepixnebart (LY3016859) using the final population PKPD model (run321). Red lines: observed fepixnebart quantiles (2.5th, 50th, 97.5th). Black lines: median of fepixnebart quantiles (2.5th, 50th, 97.5th) across simulated trials. Blue and red shaded areas: 95% of the fepixnebart quantiles (2.5th, 50th, 97.5th) across simulated trials. Red circles: observations

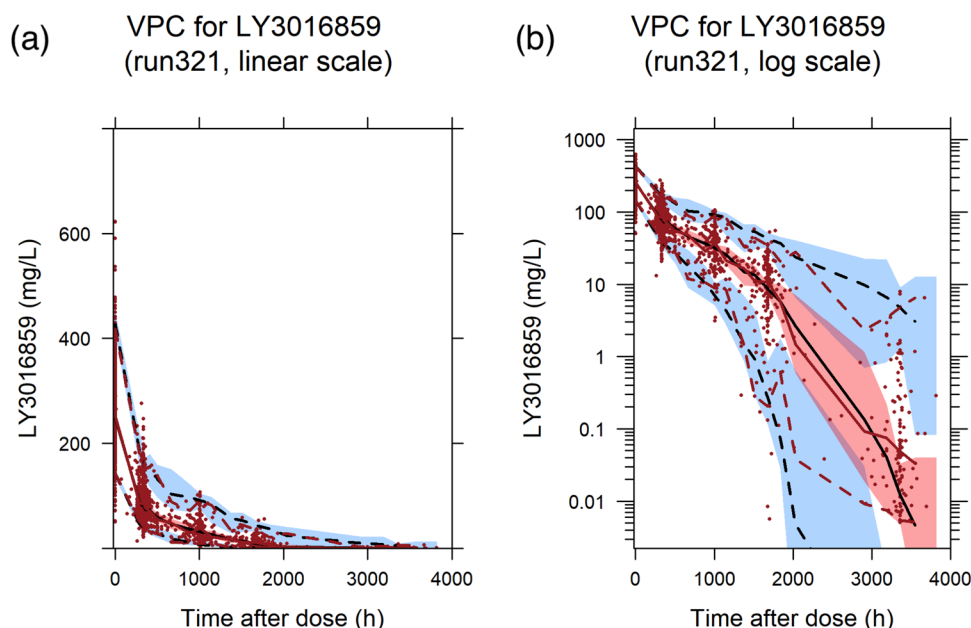
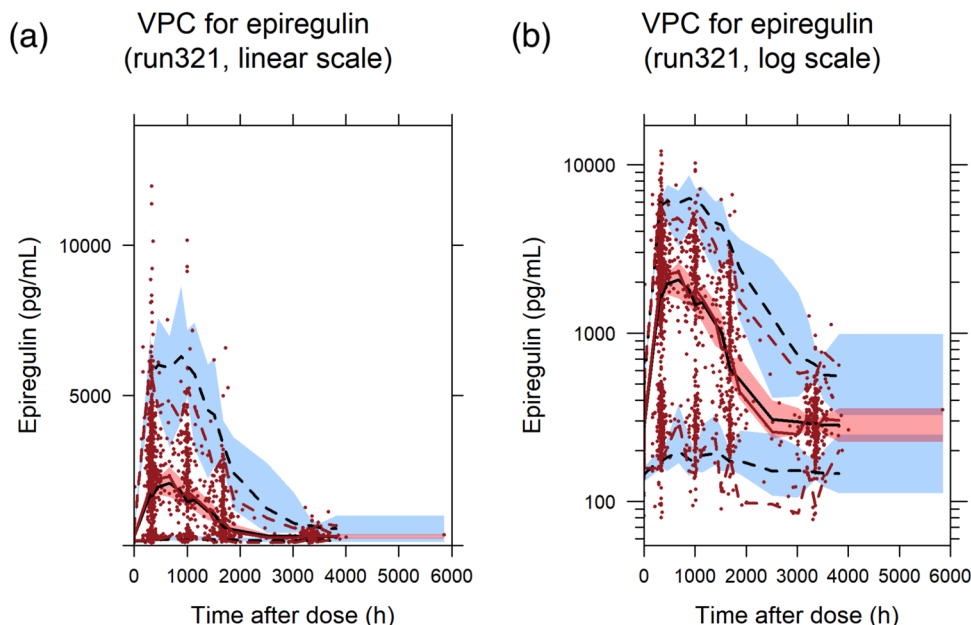


**Fig. 4** Linear scale (a) and log scale (b) of the VPC for epiregulin using the final population PKPD model (run321). Red lines: observed epiregulin quantiles (2.5th, 50th, 97.5th). Black lines: median of epiregulin quantiles (2.5th, 50th, 97.5th) across simulated trials. Blue and red shaded areas: 95% of the epiregulin quantiles (2.5th, 50th, 97.5th) across simulated trials. Red circles: observations



sufficient to test the hypothesis. A dose regimen of a 750 mg IV starting dose, followed by 500 mg Q2W, was predicted to meet the requirements.

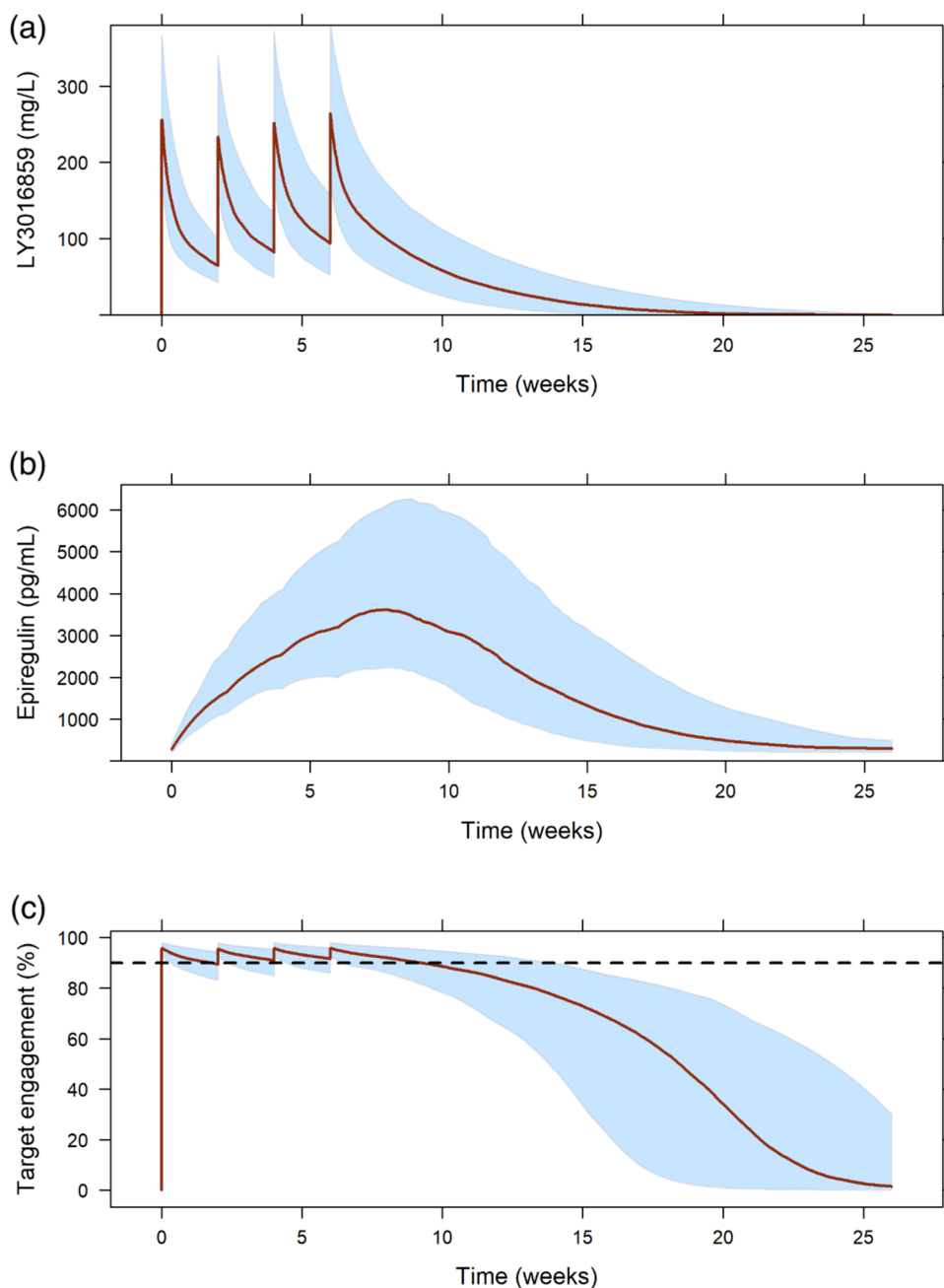
The nonlinear PK of fepixnebart was previously described by a target-mediated drug disposition model (using data from the phase 1 studies) that considers the binding equilibrium between free MAb and free target (TGF $\alpha$  and pro-epiregulin) concentrations in the central compartment as the free target and MAb-target complex turns over. The target binding process was approximated by a quasi-steady state approximation in which the binding rate was balanced by the sum of the dissociation and internalization rates. A semi-mechanistic model was

previously developed for the serum epiregulin accumulation following fepixnebart administration. In the absence of fepixnebart treatment, the epiregulin synthesis and degradation rates are in equilibrium and all epiregulin is free target with clearance via the degradation rate. When fepixnebart binds epiregulin, clearance of the fepixnebart/epiregulin complex slows down and a separate elimination rate for the fepixnebart/epiregulin complex is estimated.

The previous complex models were replaced with an alternative model for fepixnebart and epiregulin concentration versus time and comprised a parallel linear/Michaelis–Menten elimination model and an indirect



**Fig. 5** Simulated profiles of fepixnebart (a), epiregulin (b), and target engagement for the phase 2 dose regimen (c). Red line: median time profile. Blue area: 90% of the simulated concentrations (from the 5th to the 95th percentile)



response model, respectively. It was judged fit for purpose to describe the fepixnebart PK and epiregulin data collected in the phase 2 studies in OA, CLBP, and DPNP.

To estimate soluble target engagement, a PKPD model was developed for serum epiregulin accumulation following fepixnebart administration. The effect of fepixnebart on the shift of free to bound epiregulin was calculated by estimating the free fepixnebart concentration for 50% target engagement (50% clearance via degradation and 50% via the clearance of the fepixnebart/epiregulin) complex. The PKPD model was adapted for the sparsely collected data in the phase 2 studies. The Hill equation component in the phase 2 PKPD model describes the fepixnebart-induced elimination

of epiregulin. If the fepixnebart-inhibited elimination of epiregulin is assumed to be the same as the target engagement process, then the Hill equation describes fepixnebart target engagement. The predicted median target engagement confirmed that the phase 2 dose regimen achieved the required soluble target engagement of more than 90% in more than 50% of patients.

In addition to confirming adequate soluble target engagement, the covariate analysis detected that sex and GFR were significant on CL, and sex and study (disease) were significant on  $V_c$ . No effect of ADAs could be detected. Graphical analyses and VPCs indicated that

the alternative population PKPD model was appropriate to describe the available fepixnebart PK and epregeulin data.

Simulated target engagement was high throughout treatment with fepixnebart. The median simulated target engagement at week 8, 2 weeks after the last dose of fepixnebart, is predicted to be 92.0%, with 90% of predictions between 86.0% and 96.2% and with 68.5% of subjects predicted to have a target engagement of more than 90%. On the basis of simulated target engagement, the dose regimen of a 750 mg IV loading dose with a 500 mg IV maintenance dose is adequate to test the analgesic effect of fepixnebart in patients with OA, CLBP, and DPNP.

**Acknowledgements** Medical writing support was provided by Regina E. Burris, PhD, at Syneos Health.

## Declarations

**Funding** This work was funded by Eli Lilly and Company, who also sponsored the original studies, medical writing support, and open-access publication of the manuscript.

**Conflict of interest** Douglas James and Jason Bailey are full-time employees of Eli Lilly and Company and/or one of its subsidiaries and are minority holders of company stock. Jan-Stefan van der Walt, Julia Winkler, and Rik Schoemaker are full-time employees of Occams Coöperatie UA, Amstelveen, the Netherlands. At the time the study was conducted, Jan-Stefan van der Walt was a full-time employee of Eli Lilly and Company, Indianapolis, IN, USA, and was a minority holder of company stock.

**Ethics approval** All studies included in this analysis were approved by appropriate ethics committees and were conducted in accordance with the principles of the Declaration of Helsinki and the International Council on Harmonisation Good Clinical Practice guidelines.

**Consent to participate** Written informed consent was obtained from all participants of the studies included in this analysis.

**Consent for publication** Not applicable.

**Availability of data and material** Eli Lilly and Company provides access to all individual participant data collected during the trial, after anonymization, with the exception of pharmacokinetic or genetic data. Data are available to request 6 months after the indication studied has been approved in the USA and EU and after primary publication acceptance, whichever is later. No expiration date of data requests is currently set once data are made available. Access is provided after a proposal has been approved by an independent review committee identified for this purpose and after receipt of a signed data sharing agreement. Data and documents, including the study protocol, statistical analysis plan, clinical study report, and blank or annotated case report forms, will be provided in a secure data sharing environment. For details on submitting a request, see the instructions provided at [www.vivli.org](http://www.vivli.org).

**Code availability** Not applicable.

**Author contributions** J.-S.v.d.W. conceived and designed the study. J.B. was responsible for scientific oversight of immunogenicity and biomarker sample analysis. D.E.J., J.W., and R.S. analyzed the data.

D.E.J., J.-S.v.d.W., J.B., J.W., and R.S. interpreted the data. D.E.J., J.B., and J.-S.v.d.W. drafted the manuscript. J.W. and R.S. critically revised the manuscript for important intellectual content. All authors read and approved the final version of the manuscript.

**Open Access** This article is licensed under a Creative Commons Attribution-NonCommercial 4.0 International License, which permits any non-commercial use, sharing, adaptation, distribution and reproduction in any medium or format, as long as you give appropriate credit to the original author(s) and the source, provide a link to the Creative Commons licence, and indicate if changes were made. The images or other third party material in this article are included in the article's Creative Commons licence, unless indicated otherwise in a credit line to the material. If material is not included in the article's Creative Commons licence and your intended use is not permitted by statutory regulation or exceeds the permitted use, you will need to obtain permission directly from the copyright holder. To view a copy of this licence, visit <http://creativecommons.org/licenses/by-nc/4.0/>.

## References

1. Dahlhamer J, Lucas J, Zelaya C, Nahin R, Mackey S, DeBar L, Kerns R, Von Korff M, Porter L, Helmick C. Prevalence of chronic pain and high-impact chronic pain among adults—United States, 2016. *MMWR Morb Mortal Wkly Rep*. 2018;67:1001–6. <https://doi.org/10.15585/mmwr.mm6736a2>.
2. Kersten C, Cameron MG. Cetuximab alleviates neuropathic pain despite tumour progression. *BMJ Case Rep*. 2012;2012:1–6. <https://doi.org/10.1136/bcr.2011.5374>.
3. Kersten C, Cameron MG, Laird B, Mjåland S. Epidermal growth factor receptor-inhibition (EGFR-I) in the treatment of neuropathic pain. *Br J of Anaesth*. 2015;115(5):761–7. <https://doi.org/10.1093/bja/aev326>.
4. Harris RC, Chung E, Coffey RJ. EGF receptor ligands. *Exp Cell Res*. 2003;284:2–13. [https://doi.org/10.1016/s0014-4827\(02\)00105-2](https://doi.org/10.1016/s0014-4827(02)00105-2).
5. Roepstorff K, Grandal MV, Henriksen L, Knudsen SL, Lerdrup M, Grøvdal L, Willumsen BM, van Deurs B. Differential effects of EGFR ligands on endocytic sorting of the receptor. *Traffic*. 2009;10(8):1115–27. <https://doi.org/10.1111/j.1600-0854.2009.00943.x>.
6. Sloan-Lancaster J, Raddad E, Deeg MA, Eli M, Flynt A, Tumlin J. Evaluation of the safety, pharmacokinetics, pharmacodynamics, and efficacy after single and multiple dosings of LY3016859 in healthy subjects and patients with diabetic nephropathy. *Clin Pharmacol Drug Dev*. 2018;7(7):759–72. <https://doi.org/10.1002/cpdd.436>.
7. Bauer RJ (Ed) NONMEM users guide: introduction to NONMEM 7.5.0 (2017–2021). Icon Plc, Gaithersburg.
8. Lindbom L, Pihlgren P, Jonsson EN. PsN-Toolkit—a collection of computer intensive statistical methods for non-linear mixed effect modeling using NONMEM. *Comput Methods Progr Biomed*. 2005;79(3):241–57. <https://doi.org/10.1016/j.cmpb.2005.04.005>.
9. Wang W, Hallow KM, James DA. A tutorial on RxCODE: simulating differential equation pharmacometric models in R. *CPT Pharmacometr Syst Pharmacol*. 2016;5(1):3–10. <https://doi.org/10.1002/psp4.12052>.
10. Anderson BJ, Holford NHG. Mechanism-based concepts of size and maturity in pharmacokinetics. *Annu Rev Pharmacol Toxicol*. 2008;48:303–32. <https://doi.org/10.1146/annurev.pharmtox.48.113006.094708>.

11. Savic RM, Karlsson MO. Importance of shrinkage in empirical bayes estimates for diagnostics: problems and solutions. *AAPS J*. 2009;11(3):558–69. <https://doi.org/10.1208/s12248-009-9133-0>.
12. Levey AS, Bosch JP, Lewis JB, Greene T, Rogers N, Roth D. A more accurate method to estimate glomerular filtration rate from serum creatinine: a new prediction equation. Modification of diet in renal disease study group. *Ann Intern Med*. 1999;130(6):461–70. <https://doi.org/10.7326/0003-4819-130-6-199903160-00002>.
13. Lewis S, Clarke M. Forest plots: trying to see the wood and the trees. *BMJ*. 2001;322(7300):1479–80. <https://doi.org/10.1136/bmj.322.7300.1479>.
14. Karlsson MO, Holford N. A Tutorial on visual predictive checks. In: Population Approach Group Europe 2008. 2008. <http://www.page-meeting.org/?abstract=1434>. Accessed 30 Aug 2023.
15. Dosne A-G, Bergstrand M, Karlsson MO. An automated sampling importance resampling procedure for estimating parameter uncertainty. *J Pharmacokinet Pharmacodyn*. 2017;44(6):509–20. <https://doi.org/10.1007/s10928-017-9542-0>.
16. Chen YQ, Pottanat TG, Carter QL, Troutt JS, Konrad RJ, Sloan JH. Affinity capture elution bridging assay: a novel immunoassay format for detection of anti-therapeutic protein antibodies. *J Immunol Methods*. 2016;431:45–51. <https://doi.org/10.1016/j.jim.2016.02.008>.